

LAWRENCE
LIVERMORE
NATIONAL
LABORATORY

UCRL-JC-155300

Laser-Driven Hydrodynamic Experiments in the Turbulent Plasma Regime: From Omega to NIF

*H. F. Robey, A. R. Miles, J. F. Hansen, B. E.
Blue, R. P. Drake*

August 25, 2003

2003 Third International Conference on Inertial Fusion
Sciences and Applications, Monterey, CA
September 7-12, 2003

This document was prepared as an account of work sponsored by an agency of the United States Government. Neither the United States Government nor the University of California nor any of their employees, makes any warranty, express or implied, or assumes any legal liability or responsibility for the accuracy, completeness, or usefulness of any information, apparatus, product, or process disclosed, or represents that its use would not infringe privately owned rights. Reference herein to any specific commercial product, process, or service by trade name, trademark, manufacturer, or otherwise, does not necessarily constitute or imply its endorsement, recommendation, or favoring by the United States Government or the University of California. The views and opinions of authors expressed herein do not necessarily state or reflect those of the United States Government or the University of California, and shall not be used for advertising or product endorsement purposes.

This work was performed under the auspices of the U.S. Department of Energy by University of California, Lawrence Livermore National Laboratory under Contract W-7405-Eng-48.

WO19.2
**LASER-DRIVEN HYDRODYNAMIC EXPERIMENTS IN THE TURBULENT
PLASMA REGIME: FROM OMEGA TO NIF**

H.F. Robey, A.R. Miles, J. F. Hansen, B.E. Blue
LLNL, Livermore, CA, 94550, robey1@llnl.gov

R.P. Drake
University of Michigan, 2455 Hayward St., Ann Arbor, MI 48109

There is a great deal of interest in studying the evolution of hydrodynamic phenomena in high energy density plasmas that have transitioned beyond the initial phases of instability into a fully developed turbulent state. Motivation for this study arises both in fusion plasmas as well as in numerous astrophysical applications where the understanding of turbulent mixing is essential. Double-shell ignition targets, for example, are subject to large growth of short wavelength perturbations on both surfaces of the high-Z inner shell. These perturbations, initiated by Richtmyer-Meshkov and Rayleigh-Taylor instabilities, can transition to a turbulent state and will lead to deleterious mixing of the cooler shell material with the hot burning fuel.

In astrophysical plasmas, due to the extremely large scale, turbulent hydrodynamic mixing is also of widespread interest. The radial mixing that occurs in the explosion phase of core-collapse supernovae is an example that has received much attention in recent years and yet remains only poorly understood. In all of these cases, numerical simulation of the flow field is very difficult due to the large Reynolds number and corresponding wide range of spatial scales characterizing the plasma.

Laboratory experiments on high energy density facilities that can access this regime are therefore of great interest. Experiments exploring the transition to turbulence that are currently being conducted on the Omega laser will be described. We will also discuss experiments being planned for the initial commissioning phases of the NIF as well as the enhanced experimental parameter space that will become available, as additional quads are made operational.

I. INTRODUCTION AND MOTIVATION

High power lasers provide a unique platform for the study of high energy density hydrodynamic phenomena. Shock and acceleration-driven instabilities at unstable interfaces can be studied at the high Mach number, high Reynolds number conditions of interest to a wide range of phenomena ranging from astrophysics to inertial confinement fusion studies. In addition to providing the driving conditions for creating the phenomena under

study, laser-driven experiments have the unique advantage of utilizing targets that are initially solid. Therefore, interfacial perturbations seeding the instability phenomenon to be studied can be very precisely machined at interfaces between dissimilar materials. This provides very accurate control over the initial conditions for the subsequent growth of the perturbation due to instability. A large number of experiments have been conducted studying the canonical problem of the growth of single-mode sinusoidal perturbations due to both the Rayleigh-Taylor (RT) [1,2] and Richtmyer-Meshkov (RM) [3,4] instabilities.

Perturbations of more complicated modal content can also be studied. An example is shown in Figure 1, where an experimental radiograph obtained on the Omega Laser at the Laboratory for Laser Energetics is shown. The initial surface perturbation for this target consisted of two sinusoidal components with wavelengths of $\lambda_1=60\mu\text{m}$ and $\lambda_2=40\mu\text{m}$ machined into a polyimide ablator. The corresponding amplitudes of these two modes were $a_1=1.25\mu\text{m}$ and $a_2=0.75\mu\text{m}$, respectively. The ablator with the perturbed interface is assembled together with a low density ($\rho=0.1\text{g/cc}$) carbon foam cylinder in a beryllium shock tube. The deposition of 5kJ of laser energy in a 1 ns square pulse on the ablator generates a strong shock that propagates through the interface, initiating first the RM instability and then the RT instability as the interface is decelerated by the carbon foam. The perturbation has grown well into the non-linear regime due to a combination of both these instabilities.

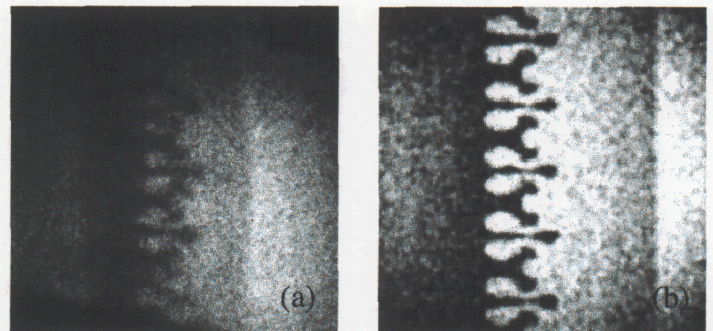


Figure 1: (a) Experimental radiograph of the shock and interfacial structure evolving from a pre-imposed two-mode sinusoidal perturbation. (b) Numerically simulated radiograph of the experiment.

Figure 1(a) shows the experimental radiograph at $t = 13\text{ns}$ obtained by backlighting the target with 4.7 keV x-rays from a Ti backlighter foil. Figure 1(b) shows the corresponding numerically simulated radiograph produced using the radiation-hydrodynamics code CALE [5]. The numerical radiograph has been post-processed with similar photon statistics to that in the experiment. Apart from the location of the shock front (which has propagated faster in the numerical simulation due to uncertainties in the equation of state of the low-density material), the agreement of the interfacial structure between the experimental and numerical radiographs is very good. Such experiments enhance the confidence in the ability of codes such as CALE to simulate the evolution of reasonably complicated perturbations well into the non-linear regime.

II. EXAMPLES OF TURBULENT PLASMAS

A. Astrophysics : Mixing in supernova simulations

While experiments such as that shown in Figure 1 are certainly useful in benchmarking code performance, there are a number of cases of interest where the hydrodynamic evolution of an unstable interface goes well beyond the initial linear and non-linear phases into the fully turbulent regime. We shall consider two such examples here.

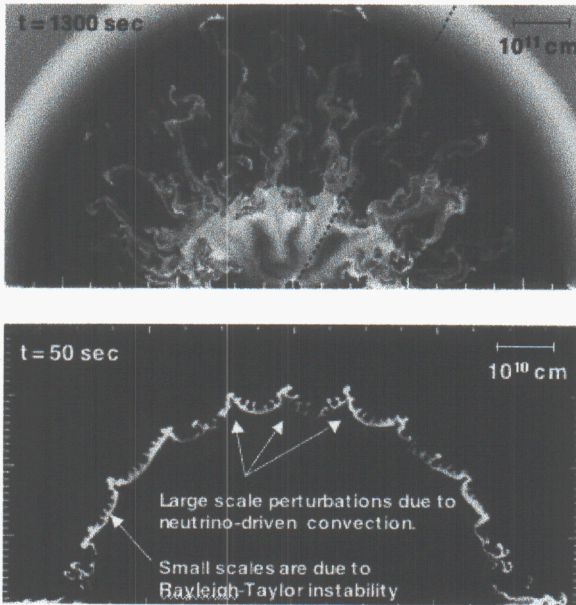


Figure 2: (a) Numerical simulation of SN 1987A by Kifonidis et al. showing outwardly propagating spikes of Fe-group elements generated by RT instability at $t=1300\text{sec}$ following core bounce. (b) Interfacial structure at $t=50\text{sec}$ initiated by neutrino-driven convection and early RT evolution.

The first example shown in Figure 2 shows an astrophysical problem of great interest. The Figure shows a

numerical simulation of the explosion phase of supernova (SN) 1987A by Kifonidis et al [6]. This particular supernova explosion was very well diagnosed observationally, and much is known about the extent of the RT-induced mixing that occurs and results in very extensive and rapid interpenetration between the interior core elements and the outer hydrogen envelope [7-9]. The extensive material interpenetration is seen in Figure 2(a), which shows spikes of Fe-group elements outwardly propagating into the lower density surrounding elements of the progenitor star at a time of 1300 seconds after core bounce. Figure 2(b) shows the same interfacial structure at earlier time, $t = 50\text{ ns}$. Here, the nature of the seed perturbation is seen. A relatively large scale perturbation arises due to neutrino-driven convection, and a smaller scale perturbation due to RT instability is seen as well.

The problem illustrated by Figure 2 is that observations of SN 1987A show clear evidence of more extensive mixing between the interior core elements and the surrounding lower density envelope than is given by any numerical simulation performed to date. The velocity of the Fe-group elements, for example, is observed to exceed 3500 km/sec by several independent sets of measurements. The velocity arising in the simulations, by contrast, is only half of this value indicating that the radial extent of the mixing is being under-predicted in the simulations.

One possible explanation for this under-prediction is that the simulations are not presently able to accurately resolve the huge range of scales, which would be present in a turbulent flow at the spatial scale and velocities characteristic of SN explosions together with estimates of the kinematic viscosity [10], the Reynolds number is found to be of the order of 10^{11} . At this exceedingly large Reynolds number, the flow should be in a turbulent state. The supernova simulations do not appear to be turbulent, however.

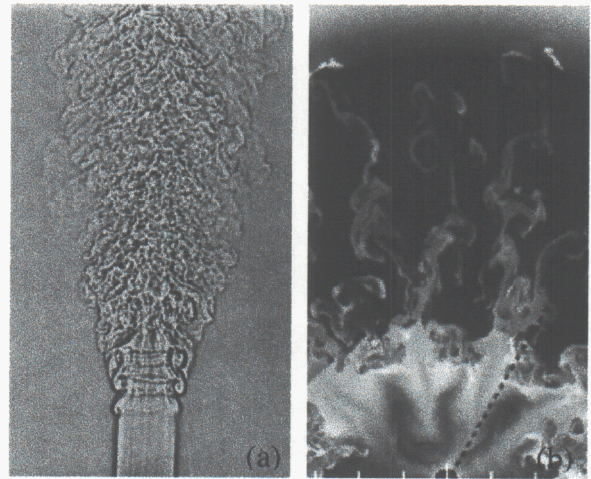


Figure 3: (a) Shadowgraph visualization of a laboratory-scale turbulent jet at $\text{Re} = 10^5$. (b) Detail of SN simulation, showing laminar filaments and regions of un-mixed material at $\text{Re} = 10^{11}$.

To illustrate this point, Figure 3 shows a comparison between (a) a laboratory-scale turbulent jet and (b) the supernova simulation of Kifonidis. The jet, visualized by shadowgraph photogra-

phy, shows an initially laminar structure, which initially becomes unstable to an axi-symmetric Kelvin-Helmholtz (KH) instability at the jet edges. A secondary instability is then seen generating a 3D azimuthal modulation related to the Widnall instability [11] superposed upon the 2D KH vortices generated by the primary instability. This sequence rather quickly and abruptly leads to a fully turbulent flow, characterized by a wide range of spatial scales. The appearance of this spectrum of scales is a defining characteristic of turbulent flows.

The SN simulation, by contrast, shows several features that are not consistent with a turbulent flow at this Reynolds number. First, as is seen in Figure 2, the modal structure has not evolved significantly from the initial seed perturbation seen at early time. A dominant perturbation with a mode number of order 24, which was seeded by the neutrino-driven convection at early time, is still clearly evident at $t = 1300$ seconds. Laminar filaments still persist as shown in Figure 3(b), with large regions of un-mixed material still present. KH instability is seen on these filaments, generating vortical roll-ups (similar to the initial phase of 2D instability in the laboratory experiment), but there is no indication of a secondary instability generating smaller scales or an interaction between the large-scale spikes and the corresponding generation of larger scales. In short, there is very little spectral development at all in the simulation.

Certainly, this is due in large part to the fact that the simulations that are presently possible are primarily two-dimensional, and the secondary instabilities that are seen in the laboratory experiment (and that are essential for the production of a fully turbulent spectrum) are not possible as they are a three-dimensional phenomenon.

The hypothesis that is suggested by this example is that in the actual supernova explosion, a transition from the initial linear and non-linear phases of RT instability to a fully developed turbulent state will give rise to a wide spectrum of spatial scales. The large scale portion of this perturbation spectrum will drive the growth of the mixing region into the self-similar regime characteristic of turbulence, with a growth rate that is much faster than the saturated non-linear growth characteristic of a spectrum of much more limited modal content.

Laboratory experiments that can produce such an instability-driven transition to turbulence in a similar high Mach number, high Reynolds number environment would be very useful for confirming this hypothesis.

B. ICF: Interfacial mixing in double-shell implosions

A second example of complex hydrodynamic phenomena in the turbulent state is found in the implosion of double-shell ICF capsules. Indirectly-driven double-shell ignition targets are being investigated as a non-cryogenic path to ignition on the National Ignition Facility (NIF). In a dou-

ble-shell target, a relatively more massive low-Z outer shell absorbs hohlraum-generated thermal x-rays and collides with a lower mass high-Z inner shell, imparting sufficient implosion velocity for volume ignition of the thermonuclear fuel. The primary function of the high-Z inner shell is to reduce radiative losses from the fuel, thus enabling lower implosion speeds. The high-Z inner shell presents a complication, however, in that it presents two interfaces with relatively large Atwood numbers that are unstable to both the RM and RT instabilities.

The extensive mixing that results at inner and outer surfaces of the inner shell is shown in Figure 4. Full details of the simulation are given in [12].

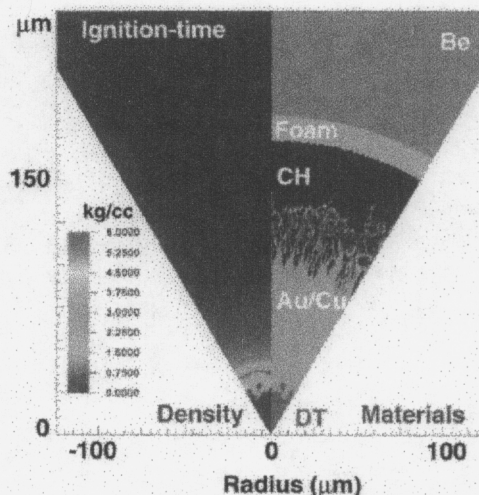


Figure 4: Numerical simulation of the implosion of a NIF-scale ignition double-shell capsule showing extensive mixing at both surfaces of the high-Z inner shell.

The velocity history that is seen by the inner surface of the inner shell is shown in Figure 5. The sequence consists of a first shock that passes through the interface giving rise to a period of relatively constant interface velocity that is RM unstable. This is then followed by a second shock, a relatively slow continued acceleration (RT stable), and a final short, but very unstable RT phase which occurs upon deceleration prior to minimum volume.

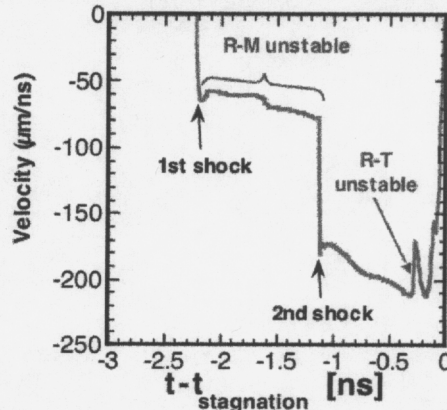


Figure 5: Velocity history of the inner surface of the high-Z inner shell.

As was the case with the SN explosion, there are questions about the ability of current numerical codes to accurately simulate the possibly turbulent mixing that occurs in such a complex acceleration history. Planar laser-driven experiments, simulating such an acceleration sequence at a diagnosable scale would be very helpful in assessing the code's performance on this very difficult problem.

III. PRESENT TURBULENT HYDRODYNAMIC EXPERIMENT CAPABILITY ON OMEGA

Experiments are currently underway on the Omega Laser to address the supernova mixing problem. The goal of these experiments is create on a laboratory scale a similar velocity history to that of the supernova, and to diagnose the evolution of a perturbed interface as it transitions beyond the linear and non-linear phases into a fully turbulent state. Once such a verifiable transition can be produced, it will then be compared with numerical simulations using astrophysical codes to assess the ability of these codes to accurately simulate the transition to turbulence.

The targets are very similar to that described earlier for the two-mode experiment of Figure 1 with the laser incident on a high density ablator and a pre-imposed perturbation machined at the interface between the ablator and a lower density material. By applying an impulsive laser drive pulse (1 ns), the interface is first rapidly accelerated by the passage of a strong shock wave and then subsequently decelerated by the lower density. The first phase is RM unstable, and the second is RT unstable as is the case in the supernova explosion. Figure 6 shows a comparison of the interface velocity histories between the full-scale and laboratory scale experiment.

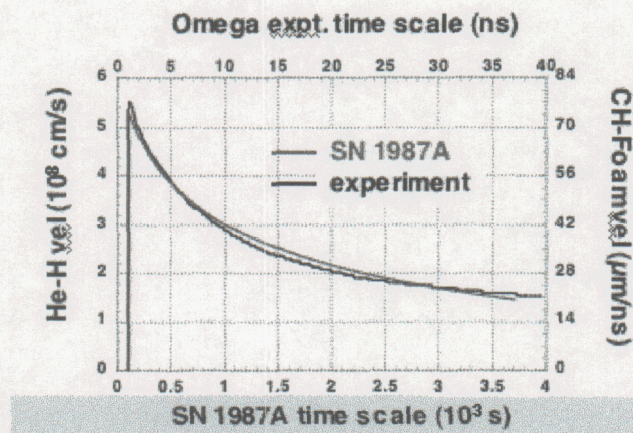


Figure 6: Comparison of the interface velocity histories between the full-scale supernova and the laboratory simulation.

This platform has been used in a wide variety of experiments by varying the perturbation at the interface. Experiments have been performed using single-mode, two-mode, 8-mode perturbations as well as two-dimensional vs. three-dimensional perturbations. In all of these cases, the interface development through the early non-linear phases was in rather good agreement with simulations [13].

In order to move the interface development further toward a transition to turbulence, a series of targets was prepared with a two-mode perturbation consisting of a rather long wave component ($\lambda_1=50\mu\text{m}$, $a_1=2.5\mu\text{m}$) with a short wavelength perturbation superposed ($\lambda_2=5\mu\text{m}$, $a_2=0.25\mu\text{m}$). In addition, as discussed in [13], the phase of the two modes differed by 90° .

The resulting evolution of this perturbation is shown in Figure 7, again visualized by x-ray radiography. Figures 7(a-c) show the interface structure at $t = 13, 25$, and 37ns , and Figure 7(d) shows, purely for qualitative comparison, the numerical simulation of Kifonidis et al. It is important to emphasize that the simulation is one of the full-scale supernova and not the laboratory experiment. A visual transition is clearly observed in the experimental radiographs from an interface structure characterized by a dominant single-mode structure at $t = 13\text{ns}$ to one that is beginning to acquire some asymmetries in the spike structure at $t = 25\text{ns}$ to one that clearly has acquired a significant range of modal components at $t = 37\text{ns}$.

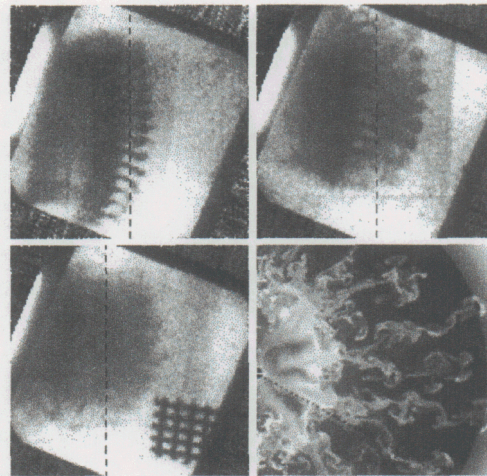


Figure 7: Experimental radiographs at (a) 13ns, (b) 25ns, and (c) 37ns of the evolution of a short-on-long wavelength perturbation exhibiting a transition to a more complicated modal structure. (d) for qualitative comparison, the Kifonidis et al. simulation of SN 1987A.

The visual "transition" observed in Figure 7 does not represent the onset of a fully developed turbulent flow, however. As discussed further in [13], there is no observed inverse cascade of energy resulting in modal components of increased spatial scale in the experiment. This is recognized quantitatively by noting that the growth rate of the mixing layer has actually decrease significantly following the transition rather than increased as would happen following transition to a self-similar turbulent layer.

The primary reason for this behavior is a limitation in the spatial scale of the experiment. With the energy available on Omega, we are limited in the transverse dimension of the experimental target that can be driven. This limitation manifests itself as a lack of planarity near the target edges with only a very narrow region remaining in the center which is unaffected by edge effects. An increase in scale would decrease the incident intensity causing a decrease in both the shock-driven RM instability and the deceleration-driven RT instability. The interface spectral evolution simply runs out of room to evolve.

A similar facility limitation is encountered in the double-shell mixing problem. Several experiments have been conducted on laser-driven facilities to study the first (RM) phase of instability [14,15] as shown in Figure 5. In order to continue the interface development with a second shock and the subsequent RT deceleration phase would require more energy delivered over a much longer time interval than that which is currently available at Omega.

IV. ENHANCED EXPERIMENTAL CAPABILITY FOR TURBULENT HYDRODYNAMICS ON NIF

At the time of this writing, NIF consists of only one single quad and is in a commissioning phase, where experimental diagnostics and techniques are being installed and tested. Very soon, however, target experiments will begin. For several years, only a planar experiment capability will exist, as the required symmetry for implosions requires a minimum beam symmetry that will not initially be available. In order to make a quantitative comparison between the present capability at Omega and that to be available soon on NIF, Table 1 lists the available energy, spatial experiment scale, and experiment duration that can be obtained with various configurations of NIF.

The drive energy is that which is available for a planar experiment, not the full system energy. For one quad of NIF, for example, this means using only 3 beams and reserving one for backlighting the experiment evolution. The second column lists the typical transverse scale of an impulsive experiment such as the supernova experiment, with the constraint being that the drive intensity remain in the range of 10^{14} - 10^{15} W/cm² to limit interface preheat effects. As the available beam energy increases, the transverse size increases as well, allowing for the appearance of an inverse cascade of energy, and the onset of fully developed turbulence. The third column relates to the ability to do an experiment similar to that described for the double-shell. This requires both increased energy in order to drive the characteristic double shocks as well as long pulse duration in order to match the specific velocity history of interest.

Laser configuration for planar experiment	Drive energy	Expt. scale for impulsive drive	Duration of long constant pulse
Omega	6kJ	800 μ m	11.5ns
NEL, 1 quad	12kJ	1.0mm	40ns*
NIF, 1 bundle	16kJ	1.5mm	40ns
NIF, 1 cluster	96kJ	2.5mm	80ns

Table 1: Comparison of drive energies and corresponding experiment spatial scale and temporal duration between Omega and NIF.

VI. ACKNOWLEDGEMENTS

This work was performed under the auspices of the U.S. Department of Energy by Lawrence Livermore National Laboratory under Contract No. W-7405-Eng-48.

VII. REFERENCES

- [1] LORD RAYLEIGH, Scientific Papers II (Cambridge, England), 200 (1900).
- [2] TAYLOR, G.I., *Proc. Roy. Soc. London, Ser. A*, **201**, p.192 (1950).
- [3] RICHTMYER, R.D., *Commun. Pure Appl. Math.* **13**, p. 297, (1960).
- [4] MESHKOV, E.E., *Izv. Acad. Sci. USSR Fluid Dynamics* **4**, p. 101, (1969).
- [5] BARTON, R.T., *Numerical Astrophysics*, (Jones & Bartlett, Boston, 1985).
- [6] KIFONIDIS, K., PLEWA, T., JANKA, & MULLER, E., *Astrophys. J.* **531**, L123 (2000).
- [7] DOTANI, T., HAYASHIDA, K., INOUE, H. et al., *Nature* **330**, p.230 (1987).
- [8] SUNYAEV, R., KANIOVSKY, A., EFREMOV, V. et al., *Nature* **330**, p.227 (1987).
- [9] ITOH, M., KUMAGAI, S. SHIGEYAMA, T., NOMOTO, K., AND NISHIMURA, J., *Nature* **330**, p.233 (1987).
- [10] RYUTOV, D.D., DRAKE, R.P., KANE, J. et al., *Astrophys. J.* **518**, p.821 (1999).
- [11] WIDNALL, S.E., BLISS, D.B., & TSAI, C., *J. Fluid Mech.* **66**(1), p.35 (1974).
- [12] MILOVICH, J.L. [6] MILOVICH, J.L., AMENDT, P.A., ROBEY, H.F. et al., *IFSA Proceedings*, TuPo2.28, (2003).
- [13] MILES, A., *IFSA Proceedings*, WO19.4, (2003).
- [14] FARLEY, D.R., PEYSER, T.A., LOGORY, L.M. et al., *Phys. Plasmas* **6**, p.4304 (1999).
- [15] GLENDINNING, S.G., BLOSTAD, J, BRAUN, D.G. et al., *Phys. Plasmas*, submitted (2003).